Control of hubless flywheel system

Pekko JAATINEN*, Risto VIITALA**, Markus MERILÄ** and Alexander SMIRNOV*
*SpinDrive Oy
Laserkatu 6, 53850, Lappeenranta, Finland
**Teraloop Oy
Ruosilantie 18, 00390, Helsinki, Finland

Abstract
The increasing global adoption of renewable energy and electric vehicles (EVs) necessitates the development of efficient energy storage systems to stabilize power grids under fluctuating demand and supply. Conventional lithium-ion batteries, though prevalent, face limitations in applications requiring frequent charge-discharge cycles, such as EV charging stations. Flywheel energy storage systems (FESS), with their rapid response, high efficiency, and minimal degradation, present a viable alternative. This study examines the design, modeling, and control of a high-speed, hubless flywheel system supported by radial active magnetic bearings (AMBs). The flywheel utilizes a carbon fiber rotor, which offers high tensile strength and lightweight properties, enabling high angular speeds and improved energy storage density. The system incorporates a vertical rotor design with passive magnetic axial support and active radial control via AMBs. A model-based control approach is employed to manage the cross-coupled system efficiently. The system is modeled using a linearized dynamic plant model that incorporates actuator bandwidth and time delay components. Robust control is achieved using the Glover-McFarlane method, allowing for frequency response shaping and disturbance rejection. Experimental validation was conducted following system commissioning, with a focus on ensuring compliance with ISO 14839 for output sensitivity. A resonance issue caused by foundation dynamics was addressed by incorporating a resonance model into the control synthesis. Post-tuning results demonstrated improved stability margins within standard limits. The study confirms the effectiveness of model-based robust control in managing the dynamic behavior of high-speed, hubless flywheel systems with radial AMBs. These results support the feasibility of deploying such systems for grid support and EV charging applications in areas with limited peak power availability.

Keywords : AMB, Control, Flywheel, Model-based, Robust, Rotordynamics

1. Introduction

The shift towards renewable energy sources on a global scale sets demand for energy storage systems (Pullen, 2019). The electrical grid must have reserve energy storage to maintain steady load levels in response to fluctuating demand and renewable energy production. The transition toward transportation electrification is part of a global shift, causing short-term demand spikes and placing extra load on the electrical grid. Traditional lithium battery-based energy storage is not optimal for frequent cyclic charge-discharge, as is the case with electric vehicle (EV) charging stations. Flywheel-based energy storage systems convert electrical energy into kinetic energy, allowing for virtually unlimited charge-discharge cycling. Other benefits of flywheel energy storage are quick response time and zero battery degradation. Flywheels can be used to even out the short peak loads to the grid, and the energy can be recharged back to the flywheel over a longer period. This enables building EV charging stations in areas with limited electrical grid peak power.

Well-designed flywheel energy storage can have 85% to 90% round-trip efficiency (Weil et al., 2020). As electrical energy is stored in the form of kinetic energy through spinning mass, it is crucial to utilize high rotational speeds and minimize friction losses. Air friction is minimized by creating a vacuum inside the flywheel unit. Bearing losses are minimized with the use of active magnetic bearings (AMB) that provide contactless and oil-free suspension.

This paper describes specific challenges of hubless rotor behavior and its control. It addresses the control synthesis approach for radial AMB in a hubless flywheel system and presents theoretical and experimental results.

2. Hubless flywheel system with radial AMBs

Maximizing the kinetic energy stored in the flywheel is the basic design goal that can most easily be achieved by using a high rotation speed, as the angular speed has a quadratic effect as

$$E_k = \frac{1}{2} I\omega^2 \tag{1}$$

where E_k is the kinetic energy, I is the inertia, and ω is the angular speed. Operating in a high-speed region sets criteria for the rotor to withstand centrifugal forces. Carbon fibre can have up to ten times higher tensile strength than structural steel and a 30-50 times higher strength-to-weight ratio. Therefore, it is a more suitable material for high-speed rotor applications (Wang et al., 2024). The flywheel system under investigation comprises a hubless thin-ring rotor that encompasses all electrical components. The footprint of the flywheel system can hence be effectively used.

The machine is positioned vertically, and the axial movement of the cylinder-shaped carbon fibre rotor is supported by passive magnets on both sides. The photograph of the hubless rotor is presented in Fig. 1a. The Picture shows the rotor construction where a carbon fibre band is wound over ring-shaped active parts. Radial movement is controlled by a pair of active magnetic bearings positioned at the top and bottom of the rotor. A cross-sectional view of the rotor, showing the actuator and sensor locations, is presented in Fig. 1b. From left to right, the first component is the displacement sensor, the second is the radial AMB, the third is a permanent magnet ring, and the motor-generator is placed in the center part of the rotor assembly. Safety bearings are used to limit rotor movement, preventing the rotor from contacting the stator's active parts. The electrical machine's nominal power is 250 kW, and it is a permanent magnet type. Additionally, biasing the radial magnetic bearings with permanent magnets has been implemented to reduce AMB copper losses.

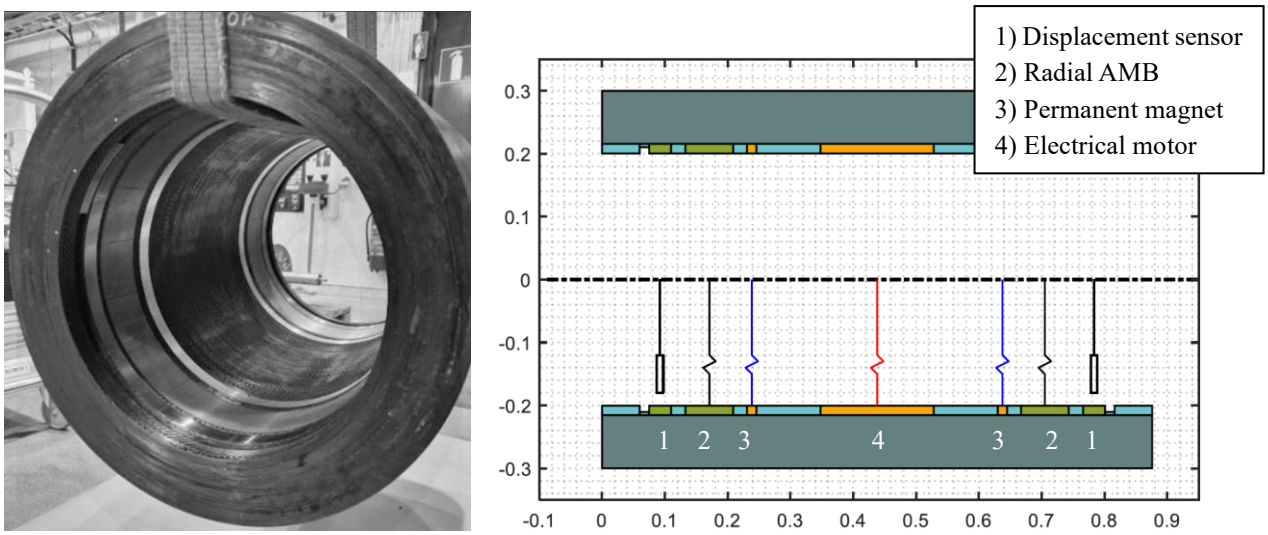

a) b)

Fig. 1. a) Photograph of the rotor, and b) sensor and actuator positions.

3. System modelling and control

This section presents the system modelling and control methods employed in the study. A model-based control approach is used to stabilize the rotor system in this machine. Consequently, the modelling principles and the control strategy are discussed in detail.

3.1 Rotordynamics

A section view of the rotodynamic model is shown in Fig. 2a. The rotor construction, made of carbon fibre material, creates a stiff rotor where the free-free mode frequencies are far above the operating range. The rotor is highly gyroscopic, as shown in Fig. 2b, where the conical model splits into backward and forward modes. Rotor speed tends to stay above the forward conical model as the polar/diametral ratio is below 1 (Genta, 2005). Additionally, the rotor expands during operation, resulting in variable magnetic gaps and thus altering the parameters of the actuators. Therefore, a robust model-based control must be designed and implemented in the magnetic bearing controller.

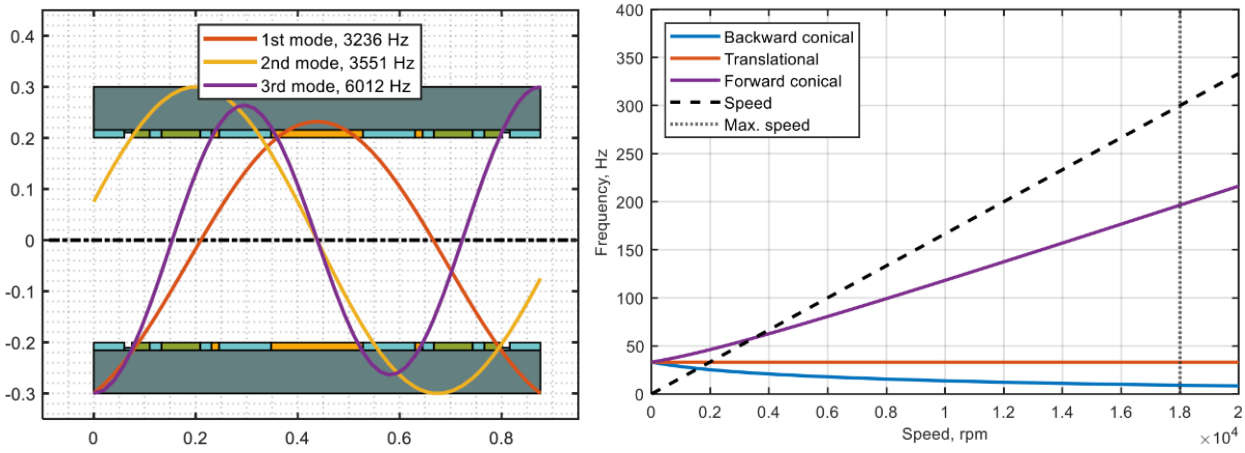

a) b)

Fig. 2. a) Free-free bending modes of the hubless rotor, and b) the Campbell diagram of the rotor.

3.2 Plant model

The plant model is formed by combining all dynamical components into a single model. This model consists of a linearized force model encompassed by the rotor model

$$\mathbf{M}\ddot{\mathbf{q}} + (\mathbf{D} + \Omega\mathbf{G})\dot{\mathbf{q}} + \mathbf{K}\mathbf{q} = \mathbf{F}, \tag{2}$$

where **M** is the mass matrix, **D** is the damping matrix, Ω is the rotation speed, **K** is the stiffness matrix, **q** is the displacement vector, and **F** is the linearized force model. The dynamics of the actuator can be modelled by its bandwidth to behave like a first-order low-pass filter

$$G_a(s) = \frac{\omega_{bw}}{s+\omega_{bw}}, \tag{3}$$

where G_a is the actuator model, s is a Laplace variable, and ω_{bw} is the actuator bandwidth in rad/s. Control systems consist of several delay components, for example, pulse-width modulation and sampling delays. Delay can be presented as

$$t_d(s) = e^{-sT}, \tag{4}$$

where t_d is time delay function is, e is Euler's number, s is a Laplace variable, and T is a time delay in seconds. Total time delay can be lumped into a single delay component in microseconds. The Padé approximation is used to create a rational function for the time delay.

3.3 Model-based control

Control tuning of a multi-input multi-output (MIMO) system can be a challenging task due to cross-couplings when using a traditional single-input single-output (SISO) system control approach, such as the PID. A robust control approach provides tools to account for uncertainties, along with loop-shaping of the frequency response. The Glover-McFarlane robust control approach was selected because it allows for an intuitive loop-shaping method for disturbance rejection in MIMO systems (Skogestad and Postlethwaite, 2001). The Glover-McFarlane method uses pre- and post-weights to shape the plant model

$$\mathbf{G}_s = \mathbf{W}_2 \mathbf{G} \boldsymbol{W}_1, \tag{5}$$

where $\mathbf{G_s}$ is the shaped plant, $\mathbf{W_2}$ is the post-compensator, $\mathbf{G}$ is the plant model, and $\mathbf{W_1}$ is the pre-compensator. The controller was synthesized using the Robust Control Toolbox, which is a part of MATLAB control tools. The post-compensator was selected to be $\mathbf{W_2} = \mathbf{I}$. With iterative control tuning, the pre-compensator value was determined to be

$$W_1 = \frac{8.9123 \cdot 10^{-4} s^2 + 1.7037 \cdot 10^3 s + 5.448 \cdot 10^3}{s^2 + 1.9117 \cdot 10^3 s + 96.8806}. \tag{6}$$

4. Experimental results

This chapter discusses the commissioning processes for the new installation of SpinDrive's Magma® X800 magnetic bearing controller, which drives magnetic bearings in the flywheel manufactured by Teraloop. System commissioning and final control tuning are described. Finally, the flywheel operation has been tested in the high-speed region.

4.1 Commissioning

The flywheel system was assembled at the end-user premises, and the initial commissioning procedure of the AMB system was conducted. The flywheel system built into the sea container, comprising two 250 kW units, is shown in Fig. 3a. This type of integrated flywheel system can be rapidly brought into service. The AMB commissioning process consists of functionality verifications, including all sensor functionality and clearance checks, as well as inner and outer control loop functionality tests.

a) b)

Fig. 3. a) Cross-section view of the machine frame, and b) container with built-in flywheel systems including two 250 kW units.

4.1 Control tuning

To ensure control system stability under disturbances, ISO 14839 specifies maximum limits for system output sensitivity (ISO 14839, 2004). For newly commissioned systems, the peak magnitude should be below 9.5 dB. A built-in identification procedure was used to determine the system's behaviour in the frequency spectrum. Output sensitivity with an initial controller is presented in Fig. 4a. It is evident that the other end of the machine exhibits a resonance peak. That resonance is caused by the foundation and frame fixing. The finite element modelling approach can be used to define foundation resonance, as by Paulsen and Santos (2020). However, using the model-based control approach, this resonance can be considered in the model

$$w_n = \frac{s+2\omega\phi+\omega^2}{s+2M\omega\phi+\omega^2}, \tag{7}$$

where ω is the frequency in rad/s, ϕ is width and M is the magnitude of the resonance. A new controller is synthesized with the resonance model, and the output sensitivity is shown in Fig. 4b. After modifications, the system stability margin complies with the standard limits.

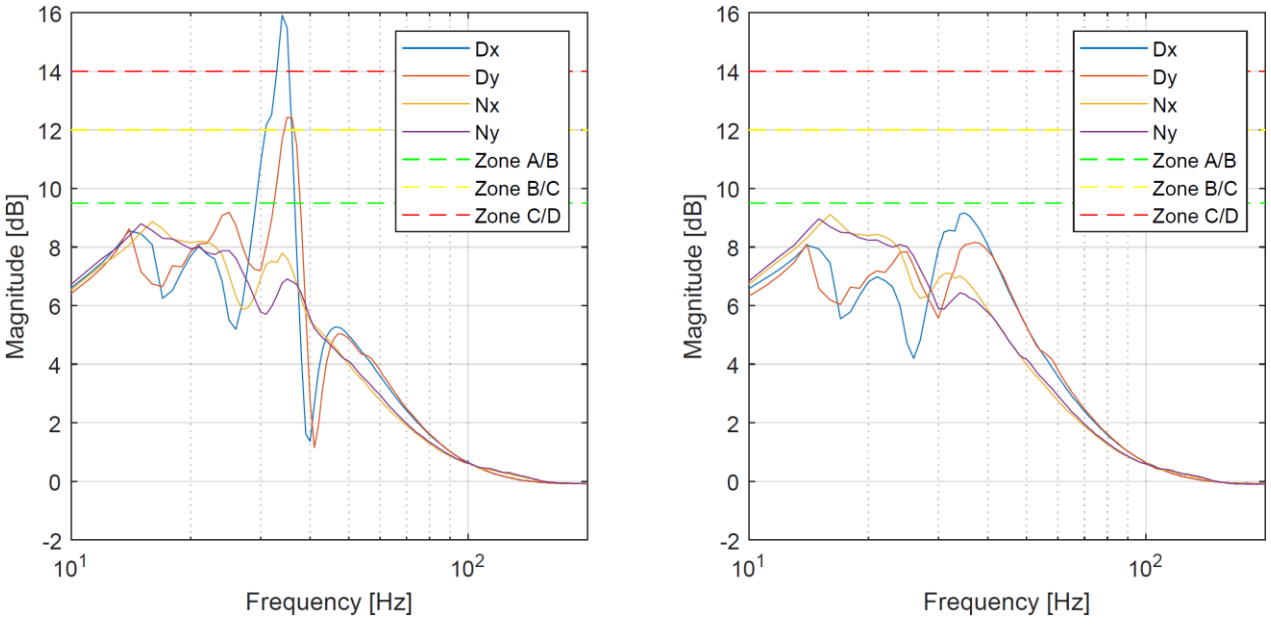

Fig. 4. System identification results show the controlled radial directions output sensitivity concerning the limits set by ISO 14839. a) Initial controller, and b) tuned controller.

4.2 Experimental test

After completion of the standstill control tuning, the dynamic testing phase begins. Speed is increased in incremental steps to observe if the controller has sufficient damping and to identify possible unmodeled resonances. The same ISO sensitivity limits are also applicable to the entire speed range. The most common sources of excessive vibrations in the higher frequency region are caused by flexible modes, rotor residual unbalance, and geometric error of the sensor surface. During dynamic testing, the rotor was successfully accelerated to 12000 r/min. From Fig. 5a, it is seen that the rotor is affected by residual unbalance. Using a synchronous notch filter, the vibration can be removed from the control loop (Herzog et al., 1996). The effect of the filter is seen in Fig. 5b. Magma X800 is equipped with a rotor balancing tool. However, this type of carbon fibre rotor structure, when operated in a vacuum, limits the possibility of conducting balancing with the magnetic bearings. In that sense, a synchronous filter must be used with this kind of system.

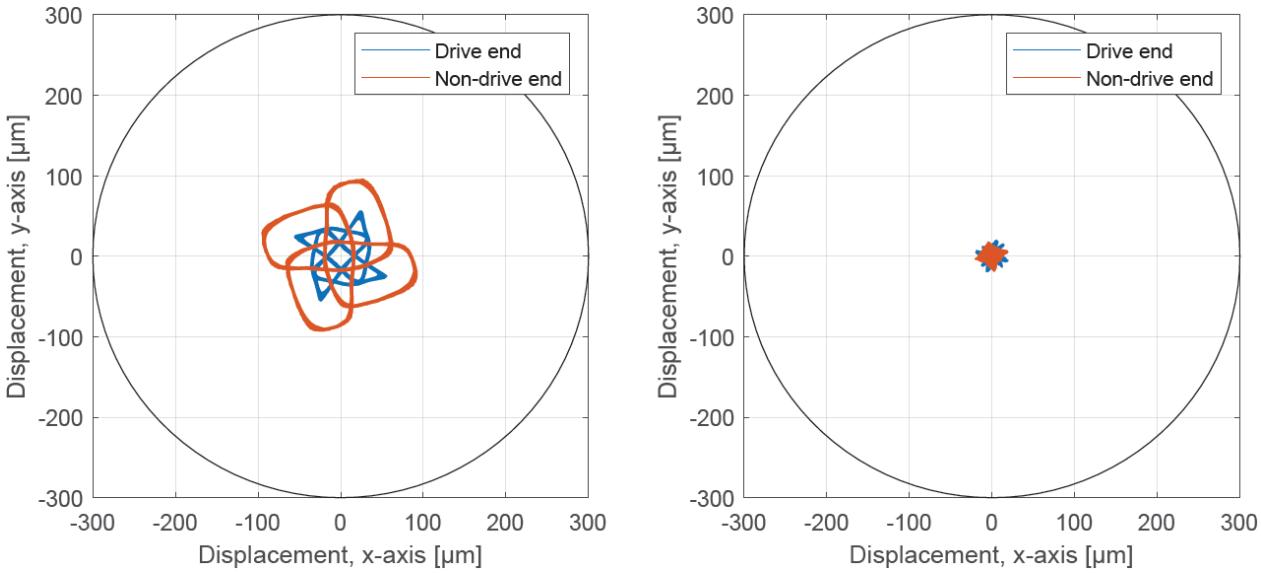

a) b)

Fig. 5. Rotor orbits at 12000 r/min, a) where the measured displacement is shown, and b) signal after synchronous filter is enabled in the feedback.

The frequency spectrum of the previous unfiltered displacement signal is calculated using the Fast Fourier Transform. Results are shown in Fig. 6. It can be noted that three frequency spikes are present, which are related to the rotor unbalance and sensor plane uncertainties. Higher harmonics are primarily related to geometric errors in the sensor plane.

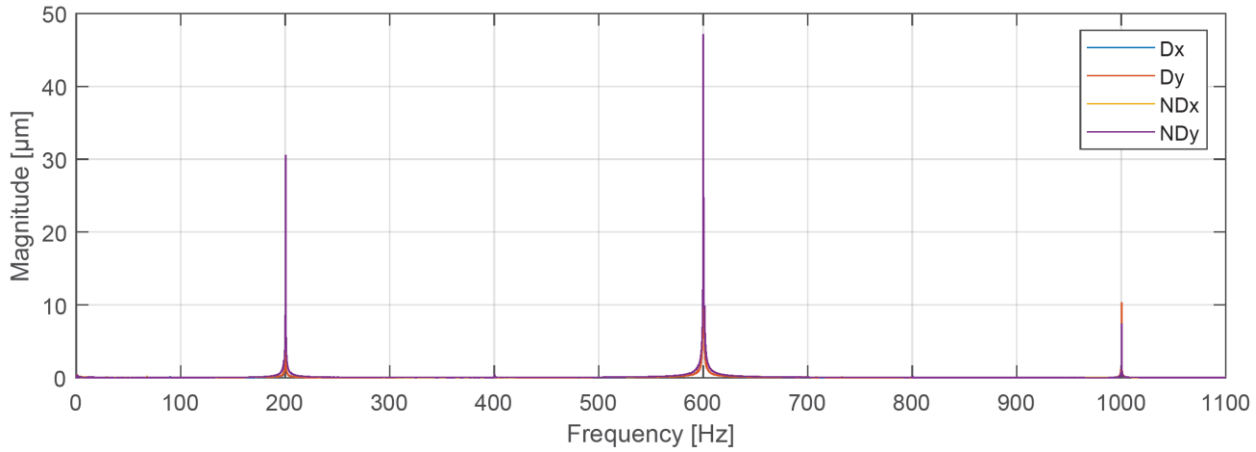

Fig. 6. Fast Fourier transformation of displacement measurement at 12000 r/min.

5. Conclusion

This study has demonstrated the feasibility and advantages of employing a high-speed, hubless flywheel energy storage system supported by radial active magnetic bearings for grid stabilization and electric vehicle charging applications.

Through detailed design and implementation, this work successfully developed a vertically oriented, magnetically supported flywheel that combines passive axial and active radial stabilization. The use of model-based robust control, particularly the Glover-McFarlane method, allowed effective handling of complex rotor dynamics, time delays, and cross-coupled MIMO system behavior. Experimental commissioning and tuning, guided by ISO 14839 standards,

confirmed the system's compliance with industrial vibration and sensitivity requirements. Notably, the incorporation of resonance modeling into the control synthesis allowed for the mitigation of structural resonances introduced by the foundation dynamics. Furthermore, the application of synchronous filters addressed residual rotor imbalance, enhancing high-speed operational stability.

In conclusion, this research validates that hubless flywheel systems with advanced control strategies for active magnetic bearings offer a scalable and efficient solution for dynamic energy storage. Their ability to respond quickly to power demand surges, without suffering from the degradation issues common in chemical batteries, makes them particularly well-suited for EV charging infrastructure and renewable grid integration. Future developments could further optimize material selection, structural dynamics, and control precision.

References

Genta, G., Dynamics of Rotating Systems. Mechanical Engineering Series. New York, NY: Springer US, (2005), pp. 105.

Herzog, R., Buhler, P., Gahler, C., and Larsonneur, R. Unbalance compensation using generalized notch filters in the multivariable feedback of magnetic bearings, in IEEE Transactions on Control Systems Technology, vol. 4, no. 5, (1996), pp. 580-586.

ISO 14839-3:2004(E) Mechanical vibration – Vibration of rotating machinery equipped with active magnetic bearings – Part 3: Evaluation of stability margin. Standard. Geneva, CH: International Organization for Standardization, (2004), pp.11-12.

Pullen, K. R., The Status and Future of Flywheel Energy Storage, Joule, vol 3, Issue 6, (2019).

Paulsen, T. T., Santos, I. F., On the foundation dynamics and the active control of flexible rotors via active magnetic bearings. In 12th International Conference on Vibrations in Rotating Machinery: Proceedings of the 12th Virtual Conference on Vibrations in Rotating Machinery (VIRM), 14-15 October, (2020). CRC Press.

Skogestad, S. and Postlethwaite, I. Multivariable feedback control analysis and design, John Wiley Sons. (2001), pp. 382-388.

Wang, Y., Wang, Z., Lv, Y., Liu, Y., Strength Analysis of Carbon Fiber Composite Flywheel Energy Storage Rotor Based on Progressive Damage Failure, Shock and Vibration, (2024).

Weil, M., Peters, J., Bauman, M. Stationary battery systems: Future challenges regarding resources, recycling and sustainability. The Material Basis of Energy Transitions (2020).